

N-Acyl Chitosan: Synthesis, Characterization and Evaluation as Sustain Released Nano Carrier for Ropinirole

Prasad R Deshmukh*, S S Khadabadi
Government College of Pharmacy, Amravati

Abstract

Chitosan was hydrophobically modified as N-Butyryl chitosan (NBC), N-Lauroyl chitosan (NLC) were synthesized and characterized by FTIR, NMR, XRD, modified chitosan were having about 14 % degree of substitution and varying solubility. Further evaluation of synthesized N-acyl chitosan to loaded ropinirole as nanoparticle by ionotropic method with crosslinking by TPP. Average particle size, drug loading, entrapment efficiency and *in-vitro* mucoadhesion of ropinirole loaded nanoparticle was 150.7 ± 3.3 nm, $24.80 \pm 1.1\%$ and $54.96 \pm 3.8\%$ respectively, with positive zeta potential which were directly correlated with increases bulkiness of the acyl substitution in the modified chitosan except zeta potential was found inversely correlated. TEM and SEM imaging relieved spherical structure of nanoparticle. In vitro release of ropinirole in 1.2 pH HCl buffer and pH 7.4 phosphate buffer showed biphasic release pattern best fitted with Korsmeyer-Peppas kinetics with fickian transport mechanism. Acylated chitosan showed sustained release reducing with increasing length of acyl group. Result of the present study showed that hydrophobically modified acylated chitosan can be useful for achieving sustained release controlled by acylation modification.

Keyword- Ionotropic Method, N-Butyryl chitosan, N-Lauroyl chitosan, Ropinirole HCl,

INTRODUCTION

Chitosan was evaluated biocompatible, biodegradable, mucoadhesive, and non-toxic natures hence more compatible to use as polymer for drug delivery [1-3].

Chitosan was prepared by deacetylation of chitin, which obtained from many natural resources viz. in cell walls of fungi, in exoskeletons of anthropods mainly in crustaceans (e.g. crabs, lobster and shrimps), insects, radulae of molluscs and in beaks and internal shells of cephalopods (e.g. octopus and squid). It having cationic in nature with linear copolymer polysaccharide made up of random distribution of β (1 \rightarrow 4) linked 2- amino- 2- deoxy- D- glucose (D-glucosamine) and 2- acetamido- 2- deoxy- D- glucose (N- acetyl-D- glucosamine) [4-6].

Chitosan having certain limitation to use as nanoparticle drug delivery include hydrophilicity and high solubility in an acidic environment, which promotes the ready degradation of the chitosan in the harsh acidic environment of the stomach, proteolytic breakdown in the gastrointestinal tract, and poor permeability across the gastrointestinal mucosa. Hence need to overcome obstacles for delivery drug effective into the blood stream and for oral administration [7].

Promoting modification such as acylation, alkylation, quaternization, thiolation, sulfation, phosphorylation, and graft copolymerization chitosan having presence of reactive amino group at C2, hydroxyl groups at C3 and C6 per glucosamine subunit [8]. Modification by hydrophobic alkyl groups onto the chitosan backbones can prompt the formation of chitosan more hydrophobic in the physiological aqueous environment. Sustain released was achieving by hydrophobically modified by cholesterol, 5 β cholanic acid, tocopherol, galactosylated O-carboxymethyl grafting with stearic acid, N-octyl-O-sulfate-modified to deliver drugs, vitamins, steroids, and proteins. [9-13].

In this study, chitosan was modified using Butyryl chloride and Lauroyl chloride and characterized using Fourier transform infrared spectroscopy (FTIR), ^1H - nuclear magnetic resonance (NMR) spectroscopy, XRD

and evaluated for solubility in solvents and degree of substitution. Ropinirole HCl loaded nanoparticles of modified N-Acyl chitosan were prepared by a ionotropic method using TPP and evaluated by particle size, zeta potential, PDI, TEM and SEM, drug loading, *In-vitro* mucoadhesion and *In-vitro* drug release was also investigated.

MATERIAL

Chitosan (55kDa; DDA 81.41%) was purchased from Merck while Butyryl chloride from sigma and Lauroyl Chloride from TCI. Ropinirole HCl was obtained as a gift sample from Glenmark Pharmaceutical Ltd (Mumbai, India). All other reagents were of analytical grade and used without further purification.

METHOD

Synthesis and Characterization of N Acyl Chitosan

For synthesis, 2.0 g chitosan was dissolved in 100 ml mixing solution of 0.6% (w/v) acetic acid solution and 85 ml of methanol. A molar equivalent (1.2) of Acyl Chloride include Butyryl chloride ($\text{C}_4\text{H}_7\text{OCl}$, Mol Wt.=106.55g) and Lauroyl Chloride ($\text{C}_{12}\text{H}_{23}\text{OCl}$, Mol Wt.=218.77g) were separately added slowly to the chitosan solution with magnetic stirring for 5 h, respectively. The mixtures were poured into the same volume of methanol and ammonia solution in volume ratio of 7 to 3. The precipitates were filtered and rinsed with distilled water, methanol, and ether. Then, they were dried in a vacuum at 50°C overnight [14].

Characterization of synthesized N-Acyl chitosans were carried out by FTIR, NMR, XRD, and evaluation of solubility in solvents and degree of Substitution using Ninhydrin Assay [15].

Preparation nanoparticles using synthesized N-Acylated chitosan

100 mg of N-Butyryl chitosan and N-Lauroyl chitosan and chitosan were separately dissolved in 40 ml of 1% acetic acid solution and 150 mg of sodium tripolyphosphate was

dissolved in 20 ml distilled water with various concentrations at pH 5, based on the results of preliminary study. 250 mg of Ropinirole HCl was dissolved in sodium tripolyphosphate solution and this solution was added drop-wise to N-acyl Chitosan solution under continuous stirring 500 RPM (Magnetic Stirrer 1L, Remi Motors Ltd. India) at room temperature [16].

Evaluation of nanoparticles

Particle Size, Zeta Potential and PDI

The lyophilized nanoparticles were dispersed in deionised water and particle size, PDI, ZP was determined by dynamic light scattering (DLS) using Zetasizer (Malvern Instrument Ltd., UK, ZS 90) monitored at a 90° angle. All measurements were made in triplicate.

% Drug loading (%DL) and % encapsulation efficiency (%EE)

Weighted ropinirole HCl loaded nanoparticles were dispersed in 10 mL of deionised water and vortexed for 5 min. The dispersion was centrifuged at 14000 rpm for 30 min and separated supernatant filtered through 0.22 µm filter (Millipore™) and analyzed at 250 nm using UV-Visible spectrophotometer (UV 2401PC, Shimadzu Corporation, Japan).

% DL and % EE were calculated using expressions previously described.

$$\% DL = \frac{\text{Amount of Ropinirole HCl in solution}}{\text{Amount of Nanoparticle}} \times 100$$

$$\% EE = \frac{\text{Amount of Ropinirole HCl in solution}}{\text{Theoretical Amount of Ropinirole added in Nanoparticle}} \times 100$$

In-vitro Mucoadhesive Study

1% (w/v) Mucin solution (1 mL) was added to each 1% w/v nanoparticle preparation (19 mL), with magnetic stirring (1L, Remi Motors Ltd. India) at 600 rpm and mixtures were incubated at 37 °C for 1 h prior to analysis. The mucin-nanoparticle mixtures were then centrifuged (C24BL, Remi Motors Ltd. India) at 1000 RPM for 60 min and 1 ml of supernatant diluted upto 10ml measured at 555 nm using UV-Visible spectrophotometer (UV 2401PC, Shimadzu Corporation, Japan) and estimate free mucin concentration using the standard calibration curve. In addition, the mucoadhesiveness was expressed as the mucin binding efficiency of the nanoparticles and was calculated from the following equation:

$$\text{Mucin Binding Efficiency \%} = \frac{C_o - C_s}{C_o} \times 100$$

Where, C_o is the initial concentration of mucin used for incubation, and C_s is the concentration of free mucin in the supernatant [17].

In-vitro Drug release study

Ropinirole HCl loaded N-Acyl chitosan and chitosan nanoparticles were performed using a dialysis bag (12-14 kDa molecular weight cutoff; Himedia, India) containing 50 ml of pH 1.2 HCl and 7.4 phosphate buffer separately. Nanoparticles of N-Acyl chitosan and chitosan comprising 1 mg equivalent Ropinirole HCl were placed in the dialysis bag and both the ends were sealed. Then, the dialysis bag was kept in the receptor compartment containing dissolution medium (pH 1.2 HCl and 7.4 phosphate buffer) at $37 \pm 0.5^\circ\text{C}$, which was stirred at 100 rpm using a magnetic stirrer (Remi Motors, India). At regular time intervals, 0.5 ml samples were withdrawn and replaced with freshly prepared buffer upto 24 h. Analyzed by spectrophotometrically at 250 nm by using a UV-Visible spectrophotometer (UV 2401PC, Shimadzu Corporation, Japan) against the blank.

RESULT AND DISCUSSION

Synthesis and Characterization of N Acyl Chitosan

The highly reactive acyl chlorides were used to react with glucosamine residue of chitosan, possess reactive amino group at C-2 position to form an amide bond. Product was precipitated with acetone and dried by lyophilization for further use (Figure 1).

IR spectroscopy N-Acyl Chitosan

The FTIR spectrum of pure chitosan exhibited the characteristic hydroxyl group absorption (3440 cm^{-1}), along with the amide I band (1647 cm^{-1}), $-\text{NH}_2$ bending (1591 cm^{-1}) and the C-O vibration (1026 cm^{-1}), while FTIR spectra of synthesized N-Acyl chitosans observed characteristic absorption peaks at $3000\text{--}3800\text{ cm}^{-1}$ for -OH and $-\text{NH}_2$ stretching vibrations, and stretching vibration intensities of $-(\text{CH}_2)_{10}-$ at $2800\text{--}2950\text{ cm}^{-1}$ and CO stretching vibration at 1068 cm^{-1} . Absorption of C-H stretching of N-Acyl chitosan at 2918 cm^{-1} and 2848 cm^{-1} increased with elongations of the alkyl side chain. Two major peaks at 1662 cm^{-1} and 1556 cm^{-1} were assigned to C=O stretching (amide I) and N-H bending vibration (amide II), respectively. Increasing amide II band in the IR spectra confirms the formation of an amide linkage between amino groups of chitosan and carboxyl groups [18]. The reaction is highly selective toward N-acylation, as it can be confirmed by the absence of a band present at 1750 cm^{-1} (Figure 2). Following observations are similar with Cho et al. who studied the acylation of chitosan using Propionic acid, hexanoic acid and stearoyl acid [14].

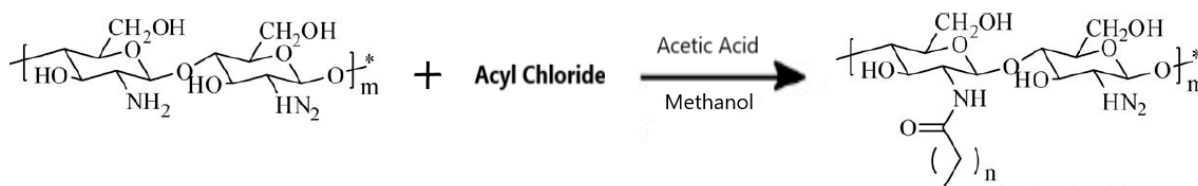


Figure 1: Synthesis Scheme for N Acyl Chitosan

Table 1: Solubilities of chitosan and N acyl chitosan in various solvents

Solvent	Chitosan	N-Butyryl Chitosan	N-Lauryl Chitosan
Water	-	+	+
Chloroform	-	+	+
Benzene	-	+	+
Toluene	-	+	+
Pyridine	-	+	+
DMSO	-	+	+
Methanol	-	+	+
Ethanol	-	+	+
Acetone	-	-	-

(+ Soluble (-) Insoluble

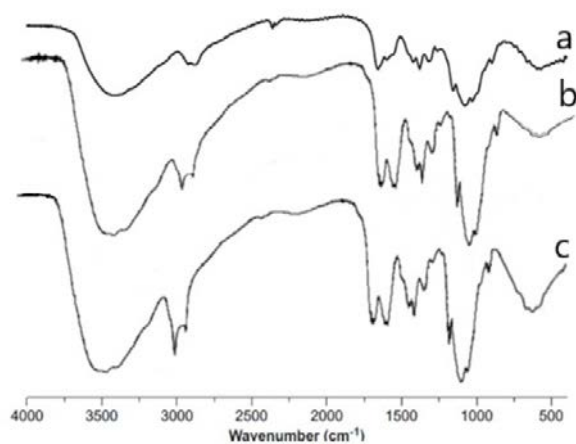


Figure 2: FTIR Spectra A (Chitosan), B (N-Butyryl chitosan), C (N-Octanoyl Chitosan), D (N-Lauroyl Chitosan) and E (N-Palmitoyl Chitosan)

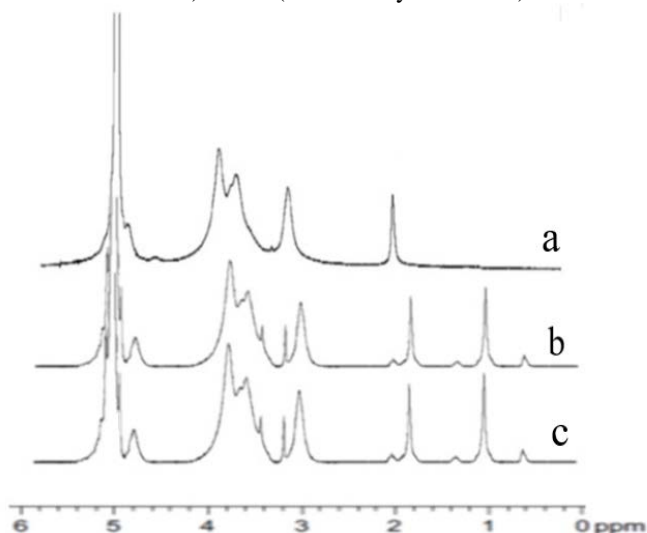
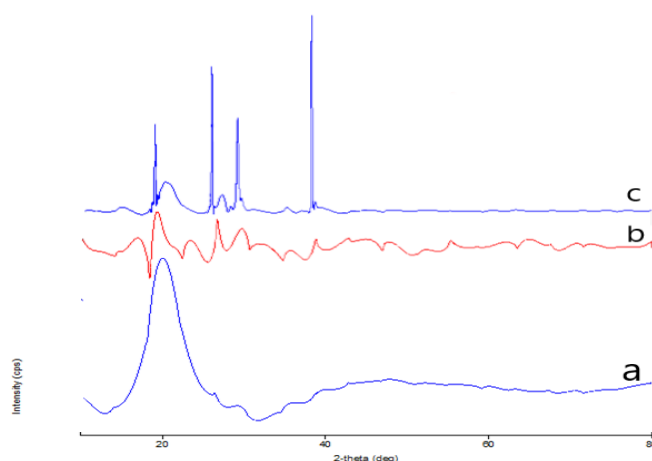
Figure 3: ¹H-NMR Spectra a (Chitosan), b (N-Butyryl chitosan), c (N-Lauroyl Chitosan)

Figure 4: XRD of a (Chitosan), b (N-Butyryl chitosan), c (N-Lauroyl Chitosan)

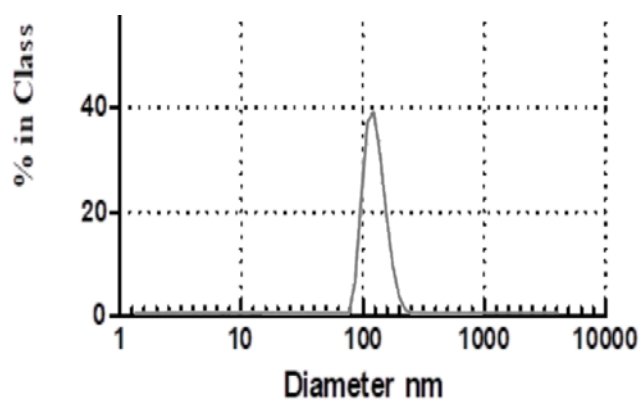


Figure 5: PDI of N Acyl Chitosan

Table 2: Zeta Potential, Particle Size and PDI

	Zeta Potential	Particle Size	PDI
Chitosan	11.9±0.6	150.7±3.3	0.396
N-Butyryl Chitosan	8.6±1.1	159.9±4.3	0.463
N-Lauroyl Chitosan	8.2±0.4	169.7±1.4	0.439

n=3

NMR of N-Acyl Chitosan

Chitosan displayed two major peaks for three N-acetyl protons of N-acetyl glucosamine and the H-2 proton of glucosamine at 1.8 ppm and 2.9 ppm. The peaks at 3.1–3.9 ppm were given for (non-anomeric) ring protons of the chitosan (H-3, H-4, H-5, and H-6). The H-1 protons of the N-acetyl glucosamine and glucosamine residues were gives peaks at 4.6 and 4.8 ppm respectively.

The $^1\text{H-NMR}$ spectrum of N-Acyl chitosan showed new peaks at 0.75 ppm for $-\text{CH}_3$ and 0.8–1.16 ppm for proton signals of $-\text{CH}_3$, 1.2–1.9 for $-\text{CH}_2-$ of acyl group, 3.0 for $-\text{CH}_3$ of acetyl group of chitosan, 3.1–3.9 CH of carbon 2 of chitosan, CH of carbon 1 of chitosan (overlapping with the ring protons) and 4.5 ppm for $-\text{CH}_2-$ (acyl protons) (Figure 3).

XRD of N-Acyl chitosan

Chitosan showed crystalline diffractions at $2\theta = 20^\circ$, while disrupted crystallinity and had been increases by the introduction of acyl substituents by modified N-Acyl chitosan (figure 4). Parallel crystallinity behavior was by Zong et al. for hexanoyl, decanoyl and lauroyl chitosan [18].

Solubility

Solubility was performing by placing 10 milligram of chitosan and N-Acyl chitosan sample into a test tube with each of 4 mL solvent. Mixing with a vortex mixer then ultrasonication, the mixture was stored at room temperature for 5 days, and visually observed as given by Ngimhuang et al [19]. High crystallinity and strong inter or intra-molecular hydrogen bonding were responsible for poor solubility of chitosan [18]. Therefore, hydrophobic substituents into chitosan backbone may likely disrupt the inter- or intra-molecular hydrogen bonding of chitosan and weaken its crystallinity. Modified acylated chitosans showed excellent solubility in common organic solvents such as halogenated hydrocarbons and aromatic solvents, but poor solubility or swelling in polar solvents also likewise showed by Jiang et al. by stearyl, palmitoyl and octanoyl chitosan [20].

Degree of Substitution

N-acyl chitosans (0.3 mg) were dissolved in an aqueous acetic acid (3% w/v, 1 mL) and thoroughly stirred. Subsequently, 0.5 mL of acetic acid/acetate buffer (4 M, pH 5.5) was added into 0.5 mL of the prepared solution. Ninhydrin reagent (1 mL) was then added and solutions were placed in a boiling water bath for 20 min. Cooled and analyzed the absorbance at 570 nm using acetic acid/acetate buffer as a blank and chitosan solution was used as a control. Ratio of absorbance by N-acyl chitosan to chitosan gives degree of substitution was found to be 12% to 14%.

Particle Size, Zeta Potential and PDI

The particle size of nanoparticles by ionotropic gelation method was ranged from 54.1 to 724.3 nm with a mean diameter of 324 nm as given by Desai and Park was prepared Protein Loading of Hexanoyl Chitosan Nanoparticles [21]. Molecular size of N-acyl was higher than chitosan resulted increases the average particle size of N-acyl chitosan moreover as the length of acyl group increase with respect to average particle size also

increases. Chitosan was cationic in nature because nanoparticle having positive zeta potential. N-acyl substituted decrease the positive charge hence having less zeta potential compared with chitosan. Along of concentration of TPP in preparation of nanoparticle also decrease of zeta potential due to the charge neutralization reaction between amine groups of chitosan and free chains and negative charges of TPP. PDI for both chitosan and N-acyl chitosan nanoparticles were ranged 0.39 to 0.45 which signified a fairly monodisperse pattern of size distribution (figure 5). The slightly increased size of N acyl chitosan could be due to its longer acyl chain group. The nanosize and spherical nature with good structural integrity of the nanoparticles was confirmed by TEM and SEM analysis (Figure 6 & 7).

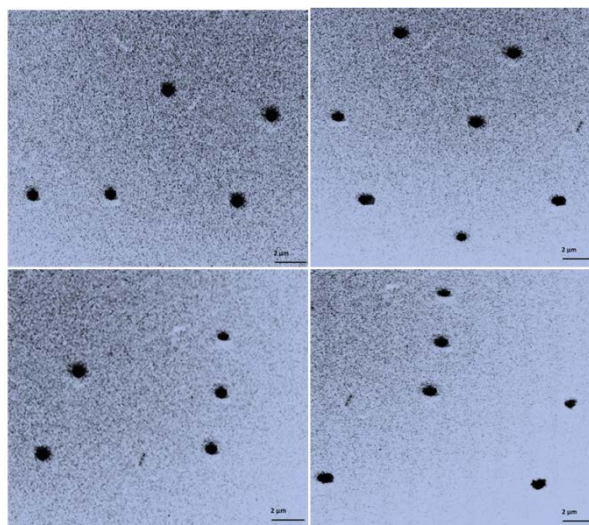


Figure 6: TEM of N Acyl Chitosan

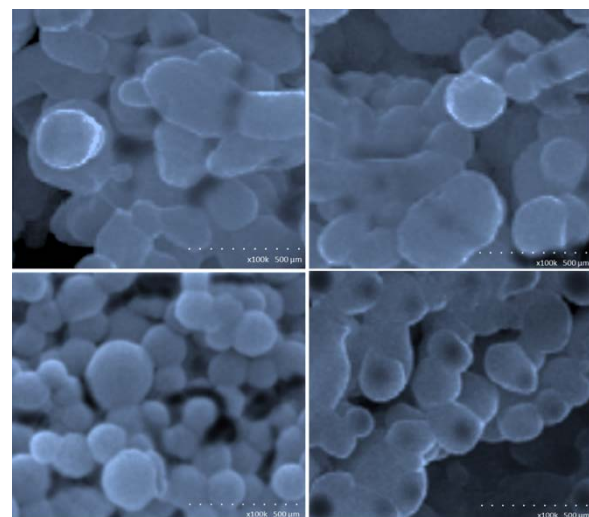


Figure 7: SEM of N Acyl Chitosan

% Drug loading (%DL) and % Encapsulation Efficiency (%EE)

Loading drugs into nanoparticles by ionotropic method was carried out by either incorporation or incubation by Agnihotri et al [22]. Drug loading capacities and EE of ionotropic chitosan nanoparticle depend on polyphosphate

crosslinker contents, chitosan-to-drug loading ratios contribute to effects EE and DL demonstrated by Amidi et al [23]. Drug was entrapment in nanoparticle matric by hydrophobic interactions, hydrogen bonding and other physiochemical forces [24, 25]. As the hydrophobic modification to chitosan by N-Acyl developed hydrogen bonding also responsible for crosslinking indirectly drug loading capacity. As increases the length of acyl group entrapment and loading get enhanced. Ropinirole HCl entrapment efficiency was increase upto 81.26±3.4 while drug loading was 28.89±1.2 as compared with chitosan (Table 3).

Table 3: % DL and % EE of Nanoparticle

	% DL	% EE
Chitosan	24.80±1.1	54.96±3.8
N-Butyryl Chitosan	25.37±1.8	62.31±4.1
N-Lauroyl Chitosan	28.89±1.2	81.26±3.4

n=3

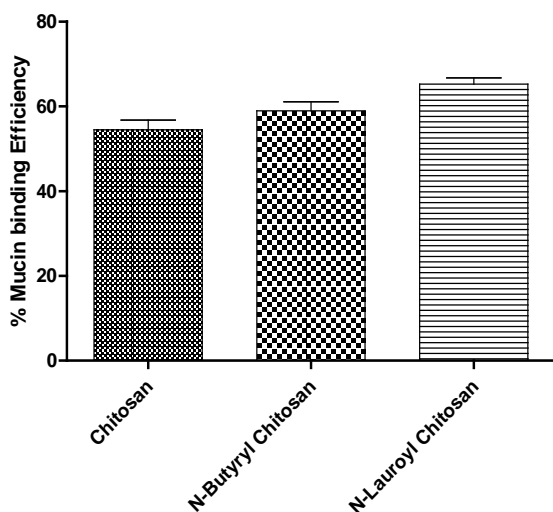


Figure 8 - %Mucin Binding Efficiency of Nanoparticle

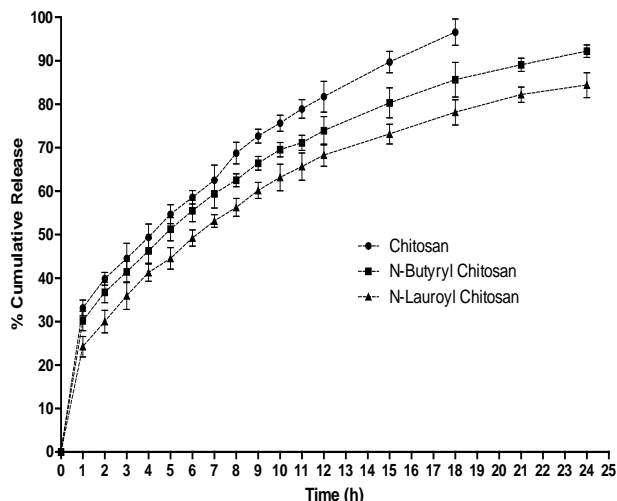


Figure 9: % Release profile at pH 1.2 of N acyl chitosan

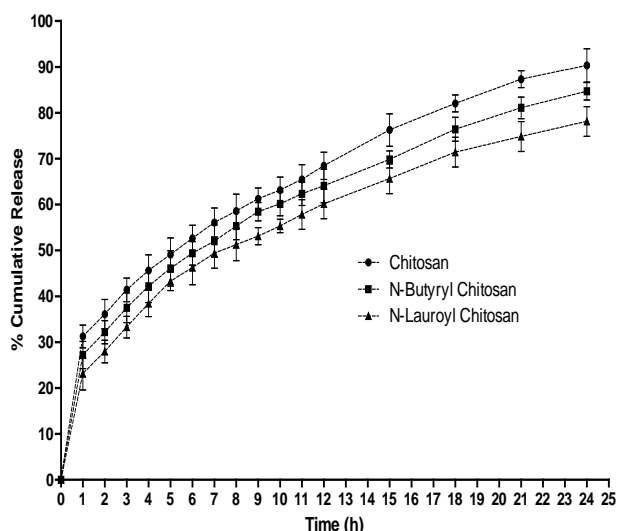


Figure 10: % Release profile at pH 7.4 of N acyl chitosan

Table 4: Release kinetics of N-Acyl Chitosan

Kinetic	Chitosan		N-Butyryl chitosan		N-Lauroyl chitosan	
	pH 1.2	pH 7.4	pH 1.2	pH 7.4	pH 1.2	pH 7.4
Zero order	0.5975	0.5674	0.6087	0.6095	0.6312	0.6566
First order	0.5979	0.5679	0.6091	0.6099	0.6316	0.6570
Higuchi	0.9890	0.9862	0.9900	0.9892	0.9919	0.9925
Peppas	0.9970	0.9963	0.9976	0.9962	0.9980	0.9970
Hixon-Crowell	0.5978	0.5678	0.6089	0.6097	0.6315	0.6568
Korsmeyer-Peppas	n	0.3960	0.4179	0.4179	0.4204	0.4398
	K	0.0263	0.0247	0.0267	0.0267	0.0230

In vitro Mucoadhesive Study

Sialic acid present in mucin is distributed throughout human tissues, is present in several fluids, including, cerebrospinal fluid, serum, urine, amniotic fluid saliva, and breast milk. Depending on the physiological conditions and physiochemical properties such as pH, the carboxylate group of sialic acid residues on mucin can interact with the positive charge on the chitosan particles, due to the protonated amino group (NH_3^+) to form electrostatic and hydrogen bonds by hydrophobic and hydrophilic interactions [26, 27]. Presence of Charge on N-acyl chitosan and chitosan nanoparticle should be estimated by zeta potential. The value of zeta potential was decreases as the attachment of acyl group. However mucin binding efficiency of N-acyl chitosan was increases with increasing the length of acyl group due to hydrogen bonds by hydrophobic interactions.

In-Vitro mucin binding efficiency can be correlated with the mucoadhesive property of nanoparticle. N-acyl substitution increases the ropinirole HCl loaded nanoparticle mucoadhesive property which directly enhanced the permission and absorption of ropinirole through the membrane. Effect of crosslinking on the N-Acyl chitosan and chitosan was observed the similar result by Hejjaji et al., who studies the effect of various chitosan:TPP concentration on mucoadhesion of Chitosan [28] (Figure 8).

In Vitro Drug release study

N-acyl chitosan and chitosan nanoparticles showed an initial burst release of ropinirole 33.13±1.84%, 30.16±2.23%, 24.22±2.34% in pH 1.2 and 31.25±2.48%, 27.19±2.96%, 23.13±3.54%, in pH 7.4 by chitosan, N-Butyryl-, N-Lauroyl chitosan nanoparticle respectively. This initial “burst effect” release is due to the fact that some amounts of ropinirole HCl was localized on the surface of nanoparticles by adsorption which could be released easily by diffusion. N-acyl chitosan was retard released due to increased hydrogen bonding with drug. Burst effect diffuse the drug which are adsorbed on surface and loosely interact with polymer and resulted 72.66±1.59%, 66.41±1.58%, 60.16±1.84% at pH 1.2 in 9 h while 68.44±2.98%, 64.06±3.65%, 60.16±3.24% at pH 7.4 in 12 h released by chitosan, N-Butyryl-, N-Lauroyl chitosan nanoparticle respectively.

Later on sustain released of the drug which are present at core diffuse slowly. Aqueous media penetrated into nanoparticle diffuse the drug. As the hydrophobic attached group to chitosan retard the penetration of media into core and enhanced the sustain release. Hydrophobicity of N-Acyl chitosan nanoparticle increase with length of acyl group with respect to its sustain release property also enhanced as 92.19±1.45% and 84.38±2.87% at pH 1.2 while 84.69±1.89% and 78.13±3.24% at pH 7.4 ropinirole released at 24 h by N-Butyryl and N-Lauroyl Chitosan respectively. While chitosan was release 96.57±3.01% at pH 1.2 after 18 h and 90.31±3.64% pH 7.4 after 24 h because of high solubility in acidic media due to protonation. Same released pattern was study by Desai and Park of Protein Loading of Hexanoyl-Modified Chitosan Nanoparticles [21] (Figure 9 & 10).

Release data of N-Acyl chitosan fitting to the Korsmeyers-Peppas model demonstrated a higher value of correlation coefficient as given in table 4. While n value $0.5 >$ for Korsmeyers-Peppas model was suggesting an fickian transport mechanism for ropinirole release by N-Butyryl-, N-Lauroyl Chitosan and Chitosan (Table 4). This suggested that the release of ropinirole from N-Acyl Chitosan nanoparticles was not only governed by diffusion, but also included polymer swelling [29]. Release kinetics by N-Acyl chitosan similar with Jafarieh et al. studies kinetics of ropinirole loaded chitosan nanoparticle prepared by ionotpic method [30].

CONCLUSION

Hydrophobically modification of chitosan was successfully done with Butyryl and Lauroyl and was characterized by FTIR, NMR, XRD evaluating successful attachment of acyl group at amino position, also improved solubility in various solvent. Ropinirole HCl was loaded efficiently in N-acyl chitosan nanoparticles by ionotropic method using TPP. Particle size of N-Acyl chitosan nanoparticle increases with length of acyl group while decreasing zeta potential was observed. PDI exhibited uniformed monodispersed particle size also proved by TEM while SEM revealed spherical particles with smooth surfaces. The loading efficiency ranged improved upto 28.89% which directly correlated to increasing the length of N-acyl side chain. N-acyl chitosan demonstrated sustain drug release at pH 1.2 and pH 7.4 as compared to chitosan. In Vitro exhibited the biphasic released pattern that followed Korsmeyers-Peppas model with $0.5 >$ n value suggesting a fickian transport mechanism.

Abbreviations

DL= Drug loading, EE= encapsulation efficiency, NBC = N-Butyryl chitosan, NLC= N-Lauroyl Chitosan

REFERENCES

- Hassan, E.E., Parish, R.C., Gallo, J.M., Optimized formulation of magnetic chitosan microspheres containing the anticancer agent, oxantazole. *Pharmaceutical Research*. 1992, 9, 390–397.
- Ohya, Y., Takei, T., Kobayashi, H., Ouchi, T. Release behavior of 5-fluorouracil from chitosan–gel microspheres immobilizing 5-fluorouracil derivative coated with polysaccharides and their cell specific recognition. *Journal of Microencapsulation*. 1993,10, 1–9.
- Tozaki, H., Komoike, J., Tada, C., Maruyama, T., Terabe, A., Suzuki, T. Chitosan capsule for colon-specific drug delivery: improvement of insulin absorption from the rat colon. *Journal f Pharmaceutical Science*. 1997, 86, 1016–1021.
- Muzzarelli, R.A.A., Boudrant, J., Meyer, D., Manno, N., DeMarchis, M., Paoletti, M.G. Current views on fungal chitin/chitosan, human chitinases, food preservation, glucans, pectins and inulin: A tribute to Henri Braconnot, precursor of the carbohydrate polymers science, on the chitin biocentennial. *Carbohydrate Polymers*. 2012, 87, 995–1012.
- Atkins, E.D.T. Conformation in polysaccharides and complex carbohydrates *J Biosci*. 1985, 8, 375–387.
- Ali, S., Ikram-uh-Haq, Qadeer, M.A., Iqbal, J. Production of citric acid by *Aspergillus niger* using cane molasses in a stirred fermentor. *Electron J Biotechn*. 2002, 5, 1-7.
- Liu, X., Chen, D., Xie, L., Zhang, R. *J Controlled Release*. 2003, 93, 93.
- Harish Prashanth, K.V., Tharanathan, R.N. Chitin/chitosan: modifications and their unlimited application potential—an overview. *Trends Food Sci. Technol*. 2007, 18, 117.

9. Wang, Y.S., Liu, L.R., Jiang, Q., Zhang, Q.Q. Self-aggregated nanoparticles of cholesterol-modified chitosan conjugates as a novel carrier of epirubicin. *Eur Polym J*. 2007, 43, 43-53.
10. Guo, H., Zhang, D., Li, C., Jia, L., Liu, G., Hao, L. Self-assembled nanoparticles based on galactosylated O-carboxymethyl chitosan-graft-stearic acid conjugates for delivery of doxorubicin. *Int. J. Pharm.* 2013, 458, 31-8.
11. Zhang, C., Qineng, P., Zhang, H. Self-assembly and characterization of paclitaxel-loaded N-octyl-O-sulfate chitosan micellar system. *Colloids Surf Biointerfaces*. 2004, 39, 69-75.
12. Quinones, J.P., Gothelf, K.V., Kjems, J., Caballero. A.M.H., Schmidt, C., Covas, C.P. N,O 6-partially acetylated chitosan nanoparticles hydrophobically-modified for controlled release of steroids and vitamin E. *Carbohydr Polym*. 2013, 91, 143-51.
13. Kim, J.H., Kim, Y.S., Kim, S., Park, J.H., Kim, K., Choi, K. Hydrophobically modified glycol chitosan nanoparticles as carrier for paclitaxel. *Journal of Control Release*. 2006, 111, 228-234.
14. Cho, Y., Kim, J.T., Park, H.J. Preparation, Characterization, and Protein Loading Properties of N-Acyl Chitosan Nanoparticles. *Journal of Applied Polymer Science*. 2012, 124, 1366-1371.
15. Curotto, E., Aros, F. Quantitative determination of chitosan and the percentage of free amino groups. *Anal Biochem*. 1993, 211, 240-241.
16. Zarifpour M, Hadizadeh F, Iman M, Tafaghodi M. Preparation and characterization of trimethyl chitosan nanospheres encapsulated with tetanus toxoid for nasal immunization studies. *Pharma Sci* 2013;18:193-8.
17. Andersen, T., Bleher, S., Eide Flaten, G., Tho, I., Mattsson, S., Škalko-Basnet, N. Chitosan in mucoadhesive drug delivery: Focus on local vaginal therapy. *Marine Drugs*. 2015, 13, 222-236.
18. Zong, Z., Kimura, Y., Takahashi, M., Yamane, H. Characterization of chemical and solid state structures of acylated chitosan. *Polymer*. 2000, 41, 899-906.
19. Ngimhuang, J., Furukawa, J., Satoh, T., Furuike, T., Sakairi, N. Synthesis of a novel polymeric surfactant by reductive N-alkylation of chitosan with 3-O-dodecyl-D-glucose. *Polymer*. 2004, 45, 837-841.
20. Jiang, G.B., Daping Quan, D., Liao, K., Wang, H. Preparation of polymeric micelles based on chitosan bearing a small amount of highly hydrophobic groups. *Carbohydrate Polymers*. 2006, 66, 514-520.
21. Desai, K.G., Park, H.J. Preparation, Characterization and Protein Loading of Hexanoyl-Modified Chitosan Nanoparticles. *Drug Delivery*. 2006, 13, 375-381.
22. Agnihotri, S.A., Mallikarjuna, N.N., Aminabhavi, T.M. Recent advances on chitosan-based micro- and nanoparticles in drug delivery. *J Control Release*. 2004, 100, 15-28.
23. Amidi, M., Mastrobattista, E., Jiskoot, W., Hennink, W.E. Chitosan-based delivery systems for protein therapeutics and antigens. *Adv Drug Deliv Rev*. 2010, 62, 159-82.
24. Ma, Z., Yeoh, H.H., Lim, L.Y. Formulation pH modulates the interaction of insulin with chitosan nanoparticles. *J. Pharm. Sci*. 2002, 91, 1396-1404.
25. Tang, E.S.K., Huang, M., Lim, L.Y. Ultrasonication of chitosan and chitosan nanoparticles. *Int. J. Pharm*. 2003, 265, 103-114.
26. Morris, G.A., Kök, S.M., Harding, S.E., Adams, G.G. Polysaccharide drug delivery systems based on pectin and chitosan. *Biotechnol Genet Eng Rev*. 2010, 27, 257-284.
27. Nikogeorgos, N., Efler, P., Kayitmazer, A.B., Lee, S. Bio-glues" to enhance slipperiness of mucins: improved lubricity and wear resistance of porcine gastric mucin (PGM) layers assisted by mucoadhesion with chitosan. *Soft Matter*. 2015, 11, 489-498.
28. Hejjaji, E.M.A., Smith, A.M., Morris, G.A. Evaluation of the mucoadhesive properties of chitosan nanoparticles prepared using different chitosan to tripolyphosphate (CS:TPP) ratios. *International Journal of Biological Macromolecules*. 2018, 120, 1610-1617.
29. Costa, P., Lobo, J. Modeling and comparison of dissolution profiles. *European Journal of Pharmaceutical Sciences*. 2001, 13, 123-133.
30. Jafarieh, O., Shadab, Md., Ali, M., Baboota, S., Sahni, J.K., Kumari, B., Bhatnagar, A., Ali, J. Design, characterization, and evaluation of intranasal delivery ropinirole-loaded mucoadhesive nanoparticles for brain targeting. *Drug Dev Ind Pharm*. 2014, 1-8.